Distribution Agreement

In presenting this thesis or dissertation as a partial fulfillment of the requirements for an advanced degree from Emory University, I hereby grant to Emory University and its agents the non-exclusive license to archive, make accessible, and display my thesis or dissertation in whole or in part in all forms of media, now or hereafter known, including display on the world wide web. I understand that I may select some access restrictions as part of the online submission of this thesis or dissertation. I retain all ownership rights to the copyright of the thesis or dissertation. I also retain the right to use in future works (such as articles or books) all or part of this thesis or dissertation.

Signature:

_____ _____

Casey Anthony Date

Dynamics of Influenza Virus Hemagglutinin Fusion Peptide Membrane Insertion

By

Casey Anthony

Master of Science

Chemistry

_____

R. Brian Dyer, Ph.D.

Advisor

_____

James Kindt, Ph.D.

Committee Member

_____

Khalid Salaita, Ph.D.

Committee Member

Accepted:

_____

Lisa A. Tedesco, Ph.D.

Dean of the James T. Laney School of Graduate Studies

_____

Date

Dynamics of Influenza Virus Hemagglutinin Fusion Peptide Membrane Insertion

Casey Anthony

Emory University, 2016

Advisor: R. Brian Dyer, Ph.D.

An abstract of

A thesis submitted to the Faculty of the

James T. Laney School of Graduate Studies of Emory University

in partial fulfillment of the requirements for the degree of

Master of Science

In Chemistry

2016

Abstract

The process of viral fusion is essential for understanding the protein4protein and protein-membrane interactions of influenza virus hemagglutinin and other analogous viral systems. The fusion peptide (FP) and the transmembrane domain (TMD) of HA2, particularly their membrane insertion and interaction, drive endosomal fusion and pore formation during the influenza virus replication process. Despite extensive studies of the hemagglutinin protein and this process, many questions surrounding FP and TMD and their mechanisms of action during membrane fusion remain. Particularly, the membrane and protein dynamics that govern these processes must be resolved.

This thesis aims to elucidate the time-resolved dynamics of fusion peptide insertion and the TMD-FP interaction. In order to probe the specific time-resolved dynamics of the TMD-FP interactions, it was necessary to first study where and at what rate the FP inserts in the membrane through equilibrium fluorescence spectroscopy and laser-induced temperature-jump spectroscopy. The data suggests that the FP inserts deeply in the membrane to at least the 10-carbon on the 16-carbon DPPC lipid chain on the microsecond timescale. In addition, the FP follows vectorial insertion in the membrane, with the N-terminus preceding the rest of the FP domain.

The last portion of this thesis begins to examine the phenomenon of J4 aggregation of NBD dye in DPPC membranes. The desegregation of J-aggregates formed from high NBD concentrations occurs in association with the gel to fluid phase transition of the membrane and can be observed through a change in fluorescence with time4resolved dynamic experiments. This is important in furthering the study of membrane dynamics.

These results will ultimately facilitate the study of the fusion peptide and its interaction with the transmembrane domain to elucidate the role of the TMD-FP complex in the membrane fusion process.

Dynamics of Influenza Virus Hemagglutinin Fusion Peptide Membrane Insertion

Casey Anthony

Emory University, 2016

Advisor: R. Brian Dyer, Ph.D.

A thesis submitted to the Faculty of the

James T. Laney School of Graduate Studies of Emory University

in partial fulfillment of the requirements for the degree of

Master of Science

In Chemistry

2016

Table of Contents

List of Figures

Chapter 1: An Introduction to Viral Membrane Proteins and Functions

1.1 Introduction

1.1.1 Dynamics of Membrane-Protein Interactions

Membrane proteins, from hormone receptors to transport proteins involved in neurotransmitter uptake, mediate numerous essential cellular functions. Understanding the complex interactions among proteins and membranes began in 1972, when Singer and Nicholson proposed the fluid mosaic membrane model. It integrates the phospholipid bilayer with peripheral and integral proteins critical to the structural integrity of the membrane, establishing the crucial role of protein-lipid interactions in a variety of membrane functions[1]. This model refuted the simplicity of the lipid bilayer and rationalized the heterogeneity of types and structures adopted by proteins. Interactions of proteins generate differentiated regions of a membrane with different thicknesses, hydrophobicity, and biological functions. Different lipid constituents throughout a membrane, including lipid rafts and glycoprotein complexes, affect lipid order and membrane rigidity, which are important to membrane structural dynamics, component mobility, and protein function.[2] While the fluid mosaic model remains the most prominent structure taught in membrane theory, new layers of complexity continue to be added to the original model to account for new observations. Models of the membrane-protein interface have been continuously developing for four decades, leading to breakthroughs in understanding the interaction between proteins and membranes and the effects of lipid structure on the function of membrane proteins, including folding and insertion. Dynamic protein-protein and protein-lipid interactions are tightly coupled with the structure and function of biological membranes.

One of the most crucial relationships between membrane and proteins is protein folding and insertion. While early two-state membrane protein folding models proposed folding of individual helices followed by intramembrane helix oligomerization[3], protein folding was soon related directly to membrane order. Changes experienced in the bilayer alters the way embedded proteins behave and fold. Booth et al. first illustrated the connection between lipids and protein folding through study of the integral membrane protein bacteriorhodopsin. Bacteriorohodopsin consists of transmembrane alpha helices that are able to refold from a denatured to native state. Through study of the protein refolding kinetics with different bending rigidities of the membrane bilayer, it was concluded that membrane rigidity results in slower rate constants for the formation of the apoprotein intermediate. This intermediate is formed before the retinal binding reaction and is the rate-limiting step for the protein folding mechanism. Lipid composition, including lipid length and rigidity, are thus directly related to membrane curvature and the force lipids induce on a protein, thereby altering its folding and behavior[4].

In addition to protein folding, the membrane-protein interface is also important for protein insertion into membranes; however, experimental methods used to study insertion either lack time resolution needed to understand the dynamics of protein insertion or the ability to couple membrane and protein dynamics. Because the pathogenicity of viral systems relies on protein insertion into membranes, elucidating the mechanisms of dynamic membrane protein interactions and insertion is crucial to understanding these systems[5].

1.1.2 Influenza Virus Hemagglutinin as a Model for Viral Fusion Mechanisms

Seasonal outbreaks and pandemics from influenza virus present significant economic burdens and public health impacts, with approximately 3 to 5 million cases and 250,000 to 500,000 deaths worldwide each year[6]. These continuous occurrences have promoted the study of influenza pathogenesis and transmissions, as well as the study of other viral systems. Hemagglutinin (HA), one of several viral coat proteins of influenza virus, is anchored to the membrane surface of the virus. It is involved in both the recognition of host cells and membrane fusion that generates a pore that releases viral genetic components into host cells. It has long served as a model for protein-mediated membrane fusion[7]. Advances in studies of hemagglutinin and its role in viral fusion have influenced our current understanding of the protein-mediated membrane fusion mechanism conserved in many analogous viral systems, including gp41 of HIV and PIV5 of parainfluenza, as well as non-pathogenic processes such as intercellular vesicle transport[8]. Understanding the mechanism of insertion and fusion will enhance design of molecules that can be used to target and insert into membranes associated with pathogenic organisms.

1.1.3 Viral Entry

Enveloped viruses attach to the cell via receptor proteins on the viral membrane, after which the virus is endocytosed into the cell. A drop in pH in the endosome instigates a conformational change in HA_2, exposing the fusion peptide to the inner endosomal membrane. After insertion into the host membrane, the fusion peptide domain forms a fusogenic unit that draws the two membranes together to form a stalk, known as the hemifusion intermediate, which ruptures to form a fusion pore through which viral RNA is released into the host cell (Figure 1)[7].

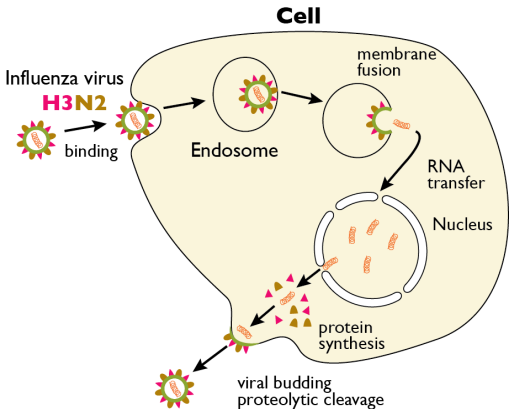

Figure 1.1. The replication cycle of Influenza A H3N2. Reprinted with permission from Hamilton, B. S.; Whittaker, G. R.; Daniel, S., Influenza virus-mediated membrane fusion: determinants of hemagglutinin fusogenic activity and experimental approaches for assessing virus fusion. *Viruses* **2012,** *4* (7), 1144-68.

1.4 Hemagglutinin Structure and Role In Protein-Mediated Fusion of Influenza Virus

The structure of hemagglutinin pre- and post-fusion has been well characterized through crystallization and NMR studies, providing insight into the different HA domains and the changes they undergo during the fusion process. The fusion-inactive precursor to fusion-active HA is cleaved at the C-terminal end to produce two functional subunits, the receptor-binding domain, HA_1, and the fusion domain, HA_2 (Figure 2).

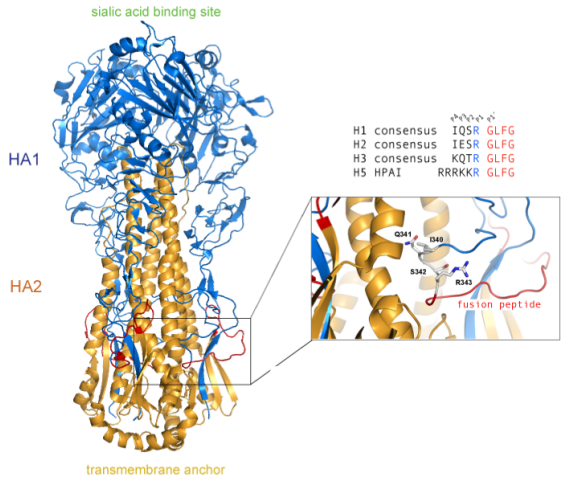

Figure 1.2. Structure of non-cleaved hemagglutinin. Reprinted with permission from Hamilton, B. S.; Whittaker, G. R.; Daniel, S., Influenza virus-mediated membrane fusion: determinants of hemagglutinin fusogenic activity and experimental approaches for assessing virus fusion. *Viruses* **2012,** *4* (7), 1144-68.

Cleavage at the surface loop of the precursor peptide is necessary to activate infectivity through a structural change to the fusion competent conformation[9]. The HA_2 domain consists of a fusion peptide (FP) domain and a transmembrane domain (TMD) that anchors the protein to the viral membrane[7]. The two are connected by a heptad repeat (HR) region consisting of a repeating sequence of seven amino acids, a pattern indicative of a coiled coil structure[10]. The entire domain functions to control membrane fusion after endocytosis.

1.5 The Fusion Peptide

The fusion peptide domain is a highly conserved 23-residue sequence of hydrophobic residues that is unstructured until it accesses the target membrane. The peptide undergoes a pH-dependent conformational change associated with insertion. At

high pH, it exists as a tight, amphipathic helical hairpin structure that favors membrane insertion over fusion (Figure 3)[11 12]. During fusion, the peptide adopts a boomerang structure stabilized by the large hydrophobic residues to become fusion active[13].

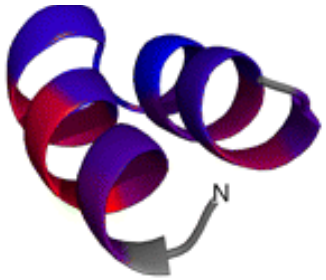

Figure 1.3. Helical hairpin structure of the fusion peptide. H1N1 sequence: GLFGAIAGFIEGGWTGMIDGWYG[GDGKKKK]. Reprinted with permission from Lorieau, J. L.; Louis, J. M.; Bax, A., The complete influenza hemagglutinin fusion domain adopts a tight helical hairpin arrangement at the lipid:water interface. *Proceedings of the National Academy of Sciences of the United States of America* **2010,** *107* (25), 11341-11346.

Trimerization of the peptide after insertion has been related to optimal fusion of the membranes through destabilization of the lipid bilayer. The FP has been postulated to promote the process of fusion stalk formation through membrane destabilization to maintain the high-energy curvature of the stalk through enhancement of negative membrane curvature[14]. According to the Tamm group, the FP inserts into the membrane in the "closed" boomerang structure[12]. At low pH, the ectodomains bring the TMD and FP into close proximity, and the outer leaflets of the viral and endosomal membranes mix in the hemifused state. Interaction between the TMD and FP is associated with the formation of the fusion pore. It was proposed that the TMD serves as a "guiding rail" for

deeper insertion of the N-terminus of the FP into the viral membrane, which further destabilizes it and facilitates fusion[15]. Study of the structure and mechanisms of the fusion peptide is important for understanding the dynamics of hemagglutinin protein and the membrane-protein interactions critical to viral pathogenicity.

*1.6 HA_2 Fusion Peptide and Transmembrane Domain Interaction*s

A model of HA_2 proposed by Chang, et al., with heptad repeat domains between the fusion peptide and TMD, prompted the exploration of the interaction between the two domains, as well as the conformation of TMD in complex with the fusion peptide in the membrane. The proposed role of TMD is twofold: it anchors the FP in the membrane, and it interacts with the FP to destabilize the membrane. Using fluorescence spectrophotometry with TMD and FP in a model membrane, key insights into the behavior of TMD in the membrane were gathered. The TMD forms the inner core of a complex with FP packed around it. At low pH, the complex was more tightly associated, and the FP was more deeply inserted. In addition, the N-terminus of the FP aligns in parallel with the C-terminus of the TMD. With these results, a model for the late steps of fusion was proposed in order to expand understanding of TMD's involvement in the hemifusion-fusion transition. After the fusion peptide inserts into the target membrane and self-associates, the HR domain pulls the two membranes together. The experiments also provided evidence for clustering of neighboring FP and TMD complexes in a conformation in which the N-terminus of the FP aligns in parallel to the C-terminus of the TMD (Figure 4)[16].

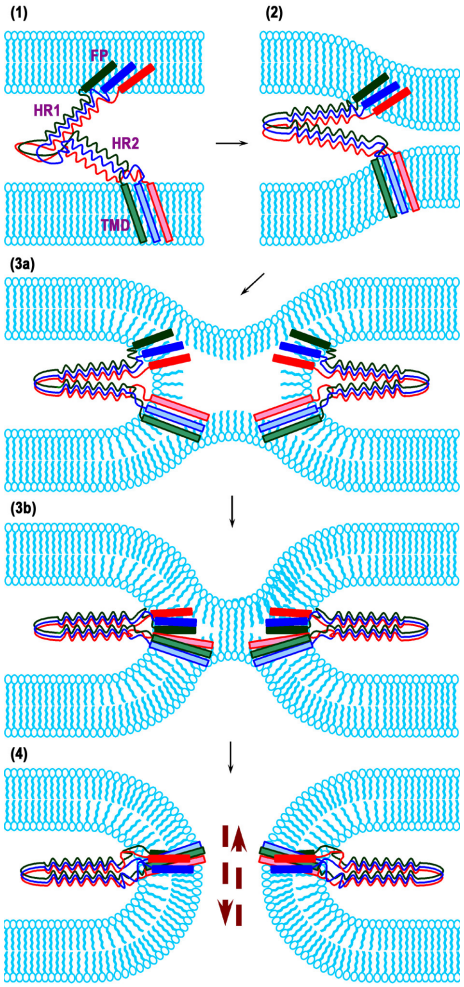

Figure 1.4. The interaction of FP and TMD during membrane fusion. (1) FP is represented by the solid lines, and TMD is represented by the lighter lines. (2) FP inserts into the target membrane. (3a) Low pH induces refolding of the HR regions to pull the two membranes together. (3b) A TMD-FP complex of a TMD core with loose FP surrounding the TMD is formed during hemifusion. (4) The hemifusion diaphragm transitions to form a pore stabilized by the TMD-FP complex. Reprinted with permission from Chang, D. K.; Cheng, S. F.; Kantchev, E. A.; Lin, C. H.; Liu, Y. T., Membrane interaction and structure of the transmembrane domain of influenza hemagglutinin and its fusion peptide complex. *BMC biology* **2008,** *6*, 2.

Most recently, it has been proposed that the TMD-FP interaction drives pore opening by increasing lipid order in the membrane, generating microdomains of order and disorder that contribute to membrane perturbation. In addition, there is evidence that the Gly1 residue on the FP N-terminus and the Ile187 residue of the TMD serve as the interaction sites for the two domains[17]. These mechanistic details of fusion raise more questions about the role of the TMD-FP complex in membrane dehydration and fusion.

1.2 Conclusions and Aim of Thesis

Despite these conclusions, there are many questions surrounding the role of the TMD-FP complex in membrane fusion, particularly around the time-resolved dynamics of FP insertion and TMD-FP interaction. The functional structures of both FP and TMD are difficult to establish due to the hydrophobicity of the peptides, the optical scattering effects of lipids, and diffusion-limited methodologies. In addition, the insertion of the FP and assembly of the HA trimer occur on an unknown timescale. Because the interaction of TMD and FP is critical to the formation of the viral fusion pore, it is important that we understand both the dynamic FP structure within the context of the membrane and the relationship between TMD and FP. It has become clear that understanding the process of viral fusion is essential to the protein-protein and protein-membrane interactions of hemagglutinin and other structures.

In order to probe specific time-resolved dynamics TMD and FP interactions, it is necessary to first study where the fusion peptide inserts in the membrane. Fusion peptide insertion depth is critical for determining the specific residues involved in the interaction of FP with TMD in the complex explained above, as well as the extent of its effect on

lipid ordering crucial to pore formation in the membrane[17]. The rate of peptide insertion is also important for understanding the energetics of the fusion process, which we can probe through dynamics experiments. By elucidating the specific fusion peptide insertion mechanism, the FP-TMD interaction and process of viral-host fusion can be further studied.

1.3 References

1. Singer, S. J.; Nicolson, G. L., The fluid mosaic model of the structure of cell membranes. *Science (New York, N.Y.)* **1972,** *175* (4023), 720-31.

2. Nicolson, G. L., The Fluid-Mosaic Model of Membrane Structure: still relevant to understanding the structure, function and dynamics of biological membranes after more than 40 years. *Biochimica et biophysica acta* **2014,** *1838* (6), 1451-66.

3. Popot, J.-L.; Gerchman, S.-E.; Engelman, D. M., Refolding of bacteriorhodopsin in lipid bilayers: A thermodynamically controlled two-stage process. *Journal of Molecular Biology* **1987,** *198* (4), 655-676.

4. Booth, P. J.; Riley, M. L.; Flitsch, S. L.; Templer, R. H.; Farooq, A.; Curran, A. R.; Chadborn, N.; Wright, P., Evidence that bilayer bending rigidity affects membrane protein folding. *Biochemistry* **1997,** *36* (1), 197-203.

5. Nagarajan, S.; Schuler, E. E.; Ma, K.; Kindt, J. T.; Dyer, R. B., Dynamics of the gel to fluid phase transformation in unilamellar DPPC vesicles. *The journal of physical chemistry.B* **2012,** *116* (46), 13749-56.

6. World Health Organization Influenza (Seasonal).

http://www.who.int/mediacentre/factsheets/fs211/en/ (accessed 13 Mar).

7. Hamilton, B. S.; Whittaker, G. R.; Daniel, S., Influenza virus-mediated membrane fusion: determinants of hemagglutinin fusogenic activity and experimental approaches for assessing virus fusion. *Viruses* **2012,** *4* (7), 1144-68.

8. Yao, H.; Lee, M. W.; Waring, A. J.; Wong, G. C.; Hong, M., Viral fusion protein transmembrane domain adopts beta-strand structure to facilitate membrane topological changes for virus-cell fusion. *Proc Natl Acad Sci U S A* **2015,** *112* (35), 10926-31.

9. Garten, W.; Bosch, F. X.; Linder, D.; Rott, R.; Klenk, H.-D., Proteolytic activation of the influenza virus hemagglutinin: The structure of the cleavage site and the enzymes involved in cleavage. *Virology* **1981,** *115* (2), 361-374.

10. Chambers, P.; Pringle, C. R.; Easton, A. J., Heptad repeat sequences are located adjacent to hydrophobic regions in several types of virus fusion glycoproteins. *The Journal of general virology* **1990,** *71 (Pt 12)*, 3075-80.

11. Lorieau, J. L.; Louis, J. M.; Schwieters, C. D.; Bax, A., Influenza Membrane Fusion as Viewed from the Structure and Dynamics of the Full-LengthHemagglutinin Fusion Domain. *Biophysical Journal* **2014,** *106* (2), 707A-707A.

12. Lai, A. L.; Tamm, L. K., Locking the Kink in the Influenza Hemagglutinin Fusion Domain Structure. *Journal of Biological Chemistry* **2007,** *282* (33), 23946 23956.

13. Lorieau, J. L.; Louis, J. M.; Schwieters, C. D.; Bax, A., pH-triggered, activated-state conformations of the influenza hemagglutinin fusion peptide revealed by NMR.

Proceedings of the National Academy of Sciences of the United States of America **2012,** *109* (49), 19994-19999.

14. Smrt, S. T.; Draney, A. W.; Lorieau, J. L., The influenza hemagglutinin fusion domain is an amphipathic helical hairpin that functions by inducing membrane curvature. *The Journal of biological chemistry* **2015,** *290* (1), 228 38.
15. Tamm, L. K., Hypothesis: spring-loaded boomerang mechanism of influenza hemagglutinin-mediated membrane fusion. *Biochimica et biophysica acta* **2003,** *1614* (1), 14-23.
16. Chang, D. K.; Cheng, S. F.; Kantchev, E. A.; Lin, C. H.; Liu, Y. T., Membrane interaction and structure of the transmembrane domain of influenza hemagglutinin and its fusion peptide complex. *BMC biology* **2008,** *6*, 2.
17. Lai, Alex L.; Freed, Jack H., The Interaction between Influenza HA Fusion Peptide and Transmembrane Domain Affects Membrane Structure. *Biophysical Journal* **2015,** *109* (12), 2523-2536.
18. Lorieau, J. L.; Louis, J. M.; Bax, A., The complete influenza hemagglutinin fusion domain adopts a tight helical hairpin arrangement at the lipid:water interface. *Proceedings of the National Academy of Sciences of the United States of America* **2010,** *107* (25), 11341-11346.

Chapter 2: Estimating H1N1 Hemagglutinin Fusion Peptide Insertion Depth Using FRET

2.1 Introduction

2.1.1 Fusion Peptide Insertion

It has been shown that the fusion peptide-transmembrane domain interaction plays a crucial role in membrane fusion through formation of a complex during hemifusion. The complex induces a highly ordered membrane structure that facilitates the transition from the hemifusion to the full fusion stage, as well as for pore opening due to aggregation of hemagglutinin that increases the concentration of FP-TMD in the pore-forming site[1]. Our objective is to probe specific TMD and FP interactions crucial to the function of HA in membrane fusion. The first step in doing this is to determine the depth and dynamics of insertion in the membrane. Accurate determination of membrane insertion depth is important for characterizing the membrane interactions of peptides, elucidating orientation, folding, or associations of a protein[2].

2.1.2 Experimental Approach

We conducted experiments on fusion peptides derived from H1N1 HA_2 to probe fusion peptide insertion depth in DPPC lipid membrane. Due to its high sensitivity and ease of application, fluorescence spectroscopy is commonly used to probe membrane peptides. In particular, the intrinsic fluorophore, tryptophan, has been widely used to probe the structure and dynamics of membrane protein folding because its fluorescence spectrum and quantum yield are sensitive to changes in the local environment from folding, oligomerization, or membrane insertion. As a result, fluorescence spectroscopy is well suited to probe peptide insertion depth. Several methods utilizing fluorescence are viable for probing insertion depth and protein-protein interactions. Forster resonance

energy transfer (FRET) can be used to measure distances between fluorophores, making it advantageous in correlating observed kinetics to specific spatial or conformational changes. The mechanism of FRET involves a donor fluorophore in its electronic excited state transferring energy to an acceptor fluorophore through non-radiative dipole-dipole interactions. The efficiency of the FRET process depends on the distance between the donor and acceptor pair, related by:

$$E_{FRET}=R_0^6/(R_0^6+r^6) \quad (1)$$

Where R_0 is the Forster radius, or the distance at which the efficiency of energy transfer is 50%. This depends on spectral overlap of the donor-acceptor pair, quantum yield of the donor, the orientation of the dipole moments, and the distance between the donor-acceptor pair. As a result, FRET is often used as a "molecular ruler"[3].

For these experiments, we use a FRET strategy that employs 4-chloro-7-nitrobenz2-oxa-1,3-diazole (NBD) on a lipid chain in a membrane as a donor and carboxytetramethylrhodamine (TAMRA) on a peptide as an acceptor. TAMRA has been used in the past to investigate the kinetics of folding and association of membrane peptides. It was shown that its fluorescence is solvent dependent, so changes in environment can be monitored as it inserts and exits the membrane. This is a known FRET pair with a Forster distance (R_0) of 5.6 nm. Due to the N-terminal arm preceding the rest of the fusion peptide insertion and serving as the site of interaction with TMD, we labeled the N-terminus with TAMRA in order to monitor location-specific insertion. Differential labeling of lipids in the DPPC vesicles with NBD at different points on the lipid chain allowed for measurement of FRET to investigate the location of the N-terminus of the fusion peptide in relation to the lipid membrane.

Previous experiments established the use of lipid phase transitions and associated changes in membrane fluidity and permeability to control peptide insertion into a lipid bilayer. Lipid membranes exhibit four distinct phases with increasing temperature: the crystal, gel, ripple, and fluid phases. The highly ordered gel phase and disordered fluid phase exhibit the sharpest transition and, as a result, the largest increase in permeability. With an increase in temperature, conversion of the lipid chains from an all-trans configuration to one with an increased number of "kinks" increases the conformational disorder of the membrane[4]. This strategy was utilized to study the insertion of FP by taking advantage of the rigid surface of a DPPC membrane in the gel phase, in which the majority of the peptide is restricted to the surface of the membrane due to the compact structure of the vesicles, and triggering FP insertion in the membrane through thermal initiation of the gel to fluid phase transition. Unilamellar DPPC vesicles were chosen as the model membrane system. With a high melting temperature of 41 ^{o}C, the phase transition occurs at a convenient temperature for use as an insertion trigger[5].

2.2 Materials and Methods

2.2.1 *Peptide Synthesis and Purification*

The H1 subtype of the HA fusion peptide, GLFGAIAGFIEGGWTGMIDGWYG[GDGKKKK], coupled to a peptide solubility tag (indicated in []), was synthesized by standard Fmoc solid phase peptide synthesis utilizing acid-amine coupling on a Liberty 1 peptide synthesizer (CEM, Matthew, NC) using a rink-amide resin. Fmoc-protected amino acids were purchased from AnaSpec, Inc. (Fremont, CA). To label the fusion peptide with 5-TAMRA, SE, purchased from

AnaSpec, Inc., at the N-terminus, labeling procedures previously outlined were followed. The succinimidyl ester (SE) on the TAMRA activates the dye for reactivity with the amino terminus. Purification of the fusion peptide was completed by HPLC on a reverse phase C18 column (Phenomenex, Torrance, CA) using a linear gradient of water and acetonitrile with 1% TFA. The mass of the peptide was confirmed by MALDI mass spectrometry using CHCA matrix dissolved in a 50:50 mixture of water and acetonitrile.

2.2.2 Circular Dichroism

The secondary structure of the peptide was confirmed using circular dichroism (CD) on a JASCO J-8- spectrophotometer equipped with a PFD-425S Jasco temperature controller (Jasco, Inc., Easton, MD). The peptide was dissolved in sodium phosphate buffer (pH 7) at a 30 μM concentration and transferred to a quartz cuvette with a 1mm path length. Instrument parameters were set to a scanning range of 190-260 nm, scan rate of 100 nm/min, response time of 2 sec, and bandwidth of 2 nm.

2.2.3 Vesicle Preparation

DPPC, 12:0 NBD PC, and 6:0 NBD PC lipids were purchased from Avanti Polar Lipids, Inc. For DPPC lipid cake preparation, DPPC in chloroform was pipetted into a 2 mL glass vial and dried with N_2 gas. The samples were then lyophilized until solvent was completely removed. For NBD PC lipid cake preparation, DPPC and NBD PC lipids in chloroform were mixed in a 100:1 ratio to generate 1% NBD PC vesicles. This was done for both the 12:0 and 6:0 NBD labeled lipids. To prepare the vesicles, the dried lipids cakes were hydrated with 20 mM sodium phosphate buffer (pH 7) at 54 ^{o}C, vortexing every 10 min for 40 min total. Small unilamellar vesicles (SUV) were prepared by sonicating the hydrated solution until it appeared clear.

2.2.4 Equilibrium FTIR

A Varian 3100 FTIR spectrometer equipped with a liquid nitrogen cooled mercury cadmium telluride (MCT) detector was used to record temperature-dependent equilibrium FTIR spectra of SUVs. The parameters were as follows: 4 scans, 2 cm^{-1} resolution, 10-80 ^{o}C temperature range every 2 ^{o}C. The DPPC and 5, 10, and 15 mol% NBD-labeled vesicles were prepared as described above in a buffer solution of 20 mM sodium phosphate and 100 mM sodium chloride in D_2O at pH 7.4. A split IR cell composed of CAF_2 windows and 126 μm spacer consisted of the reference (buffer) and the sample (lipid vesicles in buffer). The temperature of the IR cell was controlled by a water bath and measured by a thermocouple attached to the cell. The absorbance spectra were determined from the negative logarithm of the ratio of the single beam spectrum of the sample to the reference side at each temperature.

2.2.5 Equilibrium Fluorescence Emission

Equilibrium fluorescence measurements were taken with a Dual-FL spectrophotometer (Horiba Scientific, Edison, New Jersey). Total concentrations of 7.5 μM for the peptide dissolved in water and 40 μM for the vesicles were transferred to a 1 cm fluorescence cuvette for measurement. Instrument parameters were set to an integration time of 0.1 sec, 3 accumulations, and an emission coverage range of 245.61-827.74 nm. To monitor tryptophan in the fusion peptide, the excitation wavelength was set at 280 nm, while the wavelength was set at 460 nm to monitor FRET intensity between NBD and TAMRA.

2.2.5 Dynamic Light Scattering to Measure Fusion Activity

DLS measurements were taken on a Nanoplus Zeta/Nanoparticle Analyzer from Particulate Systems. Measurements were taken over a temperature range from 20-80 ^{o}C. A total concentration of 7.5 μM of peptide and 40 μM of vesicles dissolved in water were measured.

2.3 Results and Discussion

2.3.1 Effects of Fluorescent Probe NBD-PC on DPPC Structure and Phase Transition

Because the experiments rely on the gel to fluid phase transition of DPPC membranes to control peptide insertion, FTIR was used to determine the effect of the NBD label on the transition temperature at 5, 10, and 15 mol % NBD PC. Temperature-dependent data were collected every 2 ^{o}C from 10-70 ^{o}C, and the resulting spectra were analyzed in the region of the CD_2 symmetric stretch vibration of DPPC (Figure 2.1). The figure exhibits the spectrum from 15 mol% NBD PC SUVs, but spectrum from DPPC, 10 mol%, and 5 mol% yielded the similar results.

A. **B.**

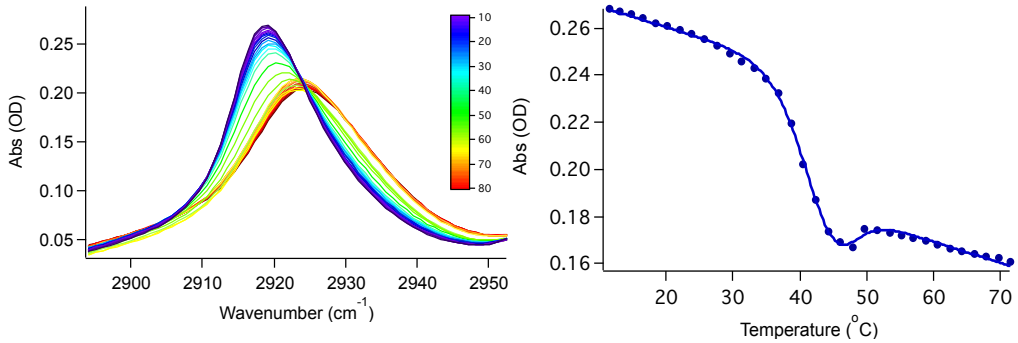

Figure 2.1. Representative temperature dependent (A) FTIR spectrum and (B) intensity vs. temperature curve of 15% NBD PC SUVs from 10-70 ^{o}C. FTIR spectrum portrays the frequency of the CD_2 symmetric stretch. The solid line represents the fit to a sigmoid equation to determine the transition temperature.

An upshift in frequency and increase in bandwidth are characteristic of the melting of the ordered gel phase to a fluid phase. The curve for unlabeled DPPC vesicles was fit to a sigmoid and yields a T_m of 41 ^{o}C, matching the literature value. DPPC vesicles with 5, 10, and 15 mol% of NBD-labeled lipids yielded a T_m of 40 ^{o}C, so the NBD fluorophore does not alter the membrane transition temperature. The melts exhibit a small transition associated with the ripple phase transition and a main phase transition associated with the ripple to fluid phase transition. The small variability in the main phase transition temperatures can be attributed to variability in vesicle radius of curvature.

2.3.2 Characterization of Fusion Peptide Secondary Structure by Circular Dichroism

Circular dichroism was performed to determine proper folding of the wild type fusion peptide into its expected α-helical conformation and define the effect of the

TAMRA label on secondary structure. For wild type FP, the spectrum in Figure 2.2 exhibits a negative peak at 197 nm in solution, indicating unfolded peptide, and peaks at 208 and 222 nm in the presence of DPPC vesicles, indicating helical structure. Folding of the FP in the presence of membrane is attributed to stabilization of the conformation through negatively charged head groups. Data collected at three temperatures indicates a temperature-dependent secondary structure that loses helicity as it approaches the melting temperature. The labeled peptide still exhibits an α-helical conformation in the presence of DPPC, suggested by the spectrum in Figure 2.2B. ; however, the peptide in solution without membrane exhibits a negative peak at 197 nm, characteristic of a β-sheet conformation. This can be attributed to the interaction of the label with hydrophobic groups near the C-terminus of the peptide, thus stabilizing a β-hairpin structure.

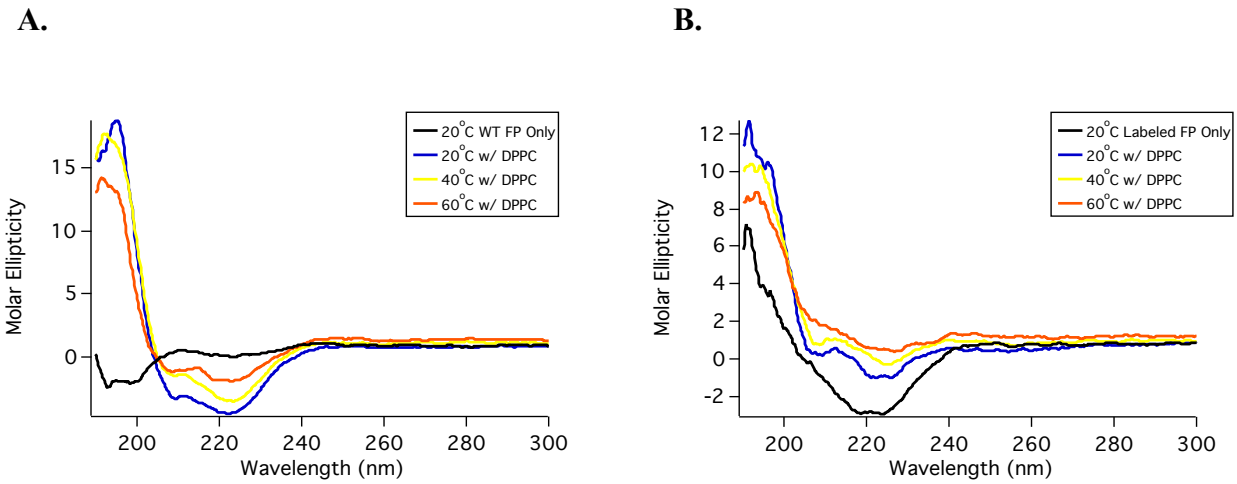

Figure 2.2. Temperature-dependent CD measurements of (A) wild-type fusion peptide with and without DPPC membrane and (B) labeled fusion peptide with and without DPPC membrane.

2.3.3 Effect of NBD-Labeled Vesicles on Fusion Peptide Insertion

Fluorescence spectroscopy was performed to determine the effects of the NBD label on fusion peptide insertion. Excitation at a wavelength of 280 nm allowed for monitoring of Trp residues as the peptide inserts. Figure 2.3A-B indicates a blue shift in emission as the temperature approaches the T_m accompanied by a small increase in intensity, both of which are associated with a more hydrophobic environment. This suggests that the peptide is burying more deeply into the membrane. The trend is followed by a red shift at higher temperatures, attributed to the peptide nearing the surface and exiting the membrane to a more hydrophilic environment. The trends observed for the wild type fusion peptide with DPPC vesicles are similar to those with NBD labeled vesicles, so it can be concluded that the NBD label has little effect on the fusion peptide's insertion into the membrane.

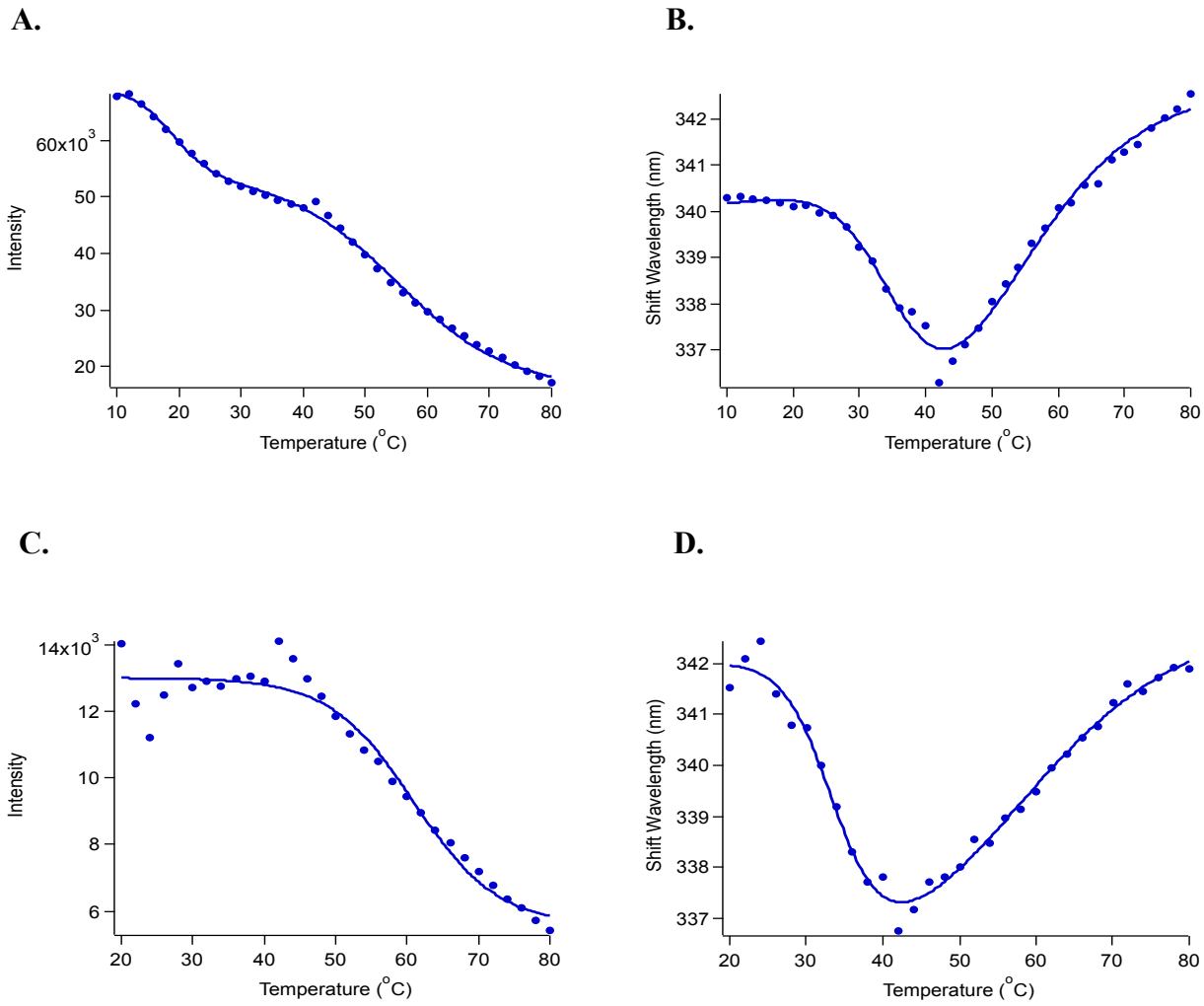

Figure 2.3. Temperature-dependent fluorescence emission from tryptophan in the wild type fusion peptide excited at 280 nm (A) Emission intensity maximum with DPPC vesicles and (B) Energy shift of maximum emission with DPPC vesicles (C) Emission intensity maximum with 1% NBD-labeled vesicles (D) Energy shift of maximum emission with 1% NBD-labeled vesicles. The curves are fit to two sigmoid curves, indicative of multiple two-state transitions as the peptide inserts and exits the membrane.

2.3.4 Effect of TAMRA Label on Membrane Insertion of the Fusion Peptide

Trends in fluorescence emission of Trp in the fusion peptide were again observed to determine the effect of the TAMRA label on fusion peptide insertion into DPPC and NBD- labeled membranes. With DPPC vesicles, the labeled fusion peptide reached a maximum blue shift at the T_m, as observed with the wild type fusion peptide; however, the subsequent red shift is not as sharp as the wild type peptide. Insertion of the labeled fusion peptid e into NBD-labeled vesicles followed the same trend below the T_m, but there is no red shift following the T_m (Figure 2.4).

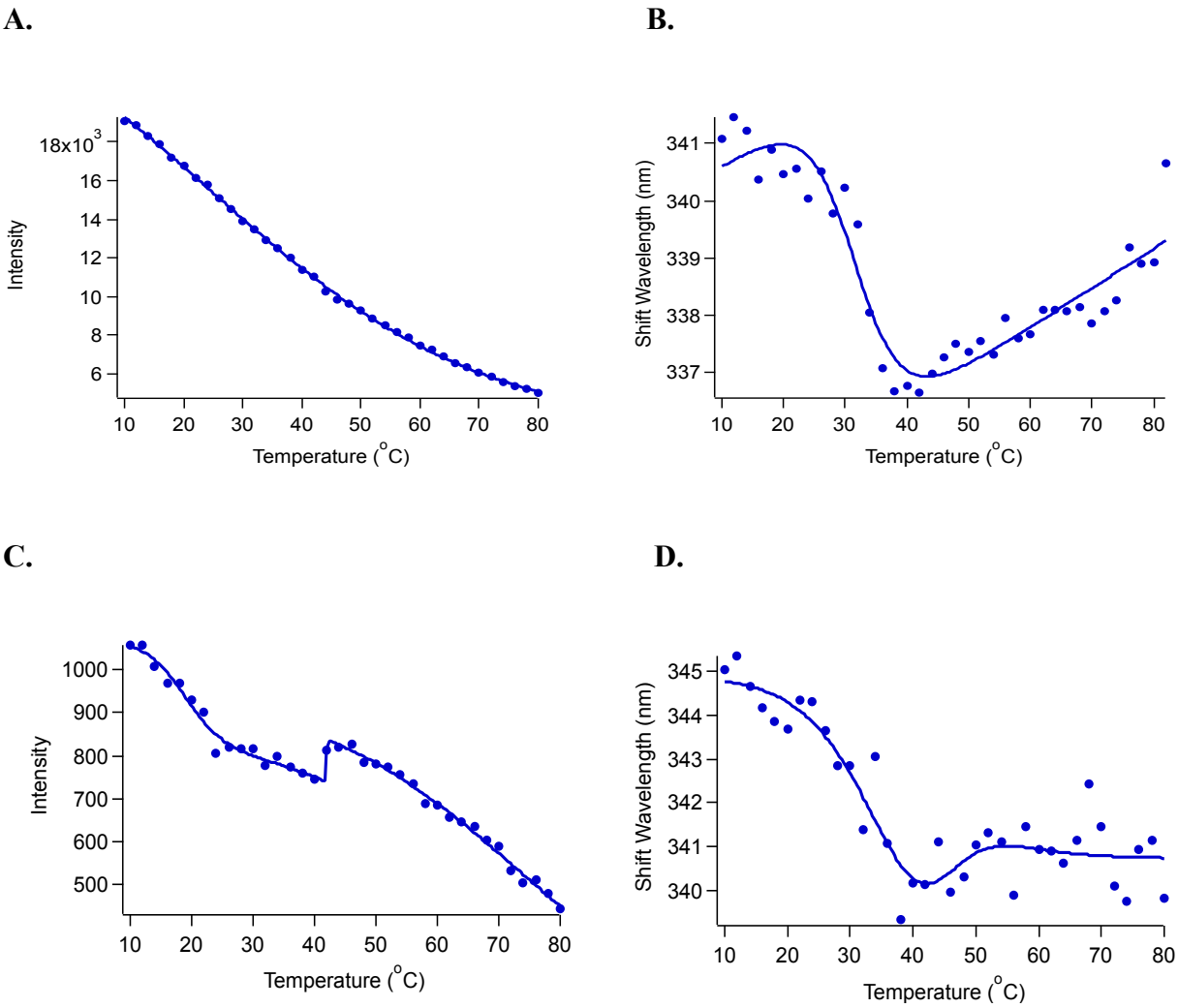

Figure 2.4. Temperature-dependent fluorescence emission from tryptophan in the TAMRA-labeled fusion peptide excited at 280 nm (A) Emission intensity maximum with DPPC vesicles (B) Energy shift with DPPC vesicles (C) Emission intensity maximum with NBD-labeled vesicles (D) Energy shift with NBD-labeled vesicles.

This suggests that the bulky fluorophores cause the peptide to remain in the membrane once it inserts due to favorable hydrophobic associations between TAMRA and the inner membrane.

2.3.5 Fusion Activity of Wild Type and Labeled Fusion Peptide

[1]Experiments with mutant fusion peptides have shown that wild type FP peptides exhibit only hemifusion activity, while mutating the N-terminus position abolishes fusion altogether. As shown in Figure 2.5A-B, the vesicles themselves are 50-100 nm in size, confirming the presence of SUVs. Dynamic light scattering measures the diffusion rate of the vesicles to estimate the size distribution profile of a population of particles. The average diffusion rate appears to decrease with the addition of peptide to the DPPC vesicles, corresponding to the peptides associating with the membranes. The average diffusion rate of the population increases above the T_m of the membrane, indicating a change in the water structure at the liquid-membrane interface. Figure 2.5A suggests hemifusion activity after the peptide inserts into the membrane at a temperature above the T_m of the membrane, indicated by the formation of populations much larger in diameter. Figure 2.5B shows no formation of populations of larger vesicles. Both of these results correspond to literature predictions of fusion activity of the wild type and labeled peptides.

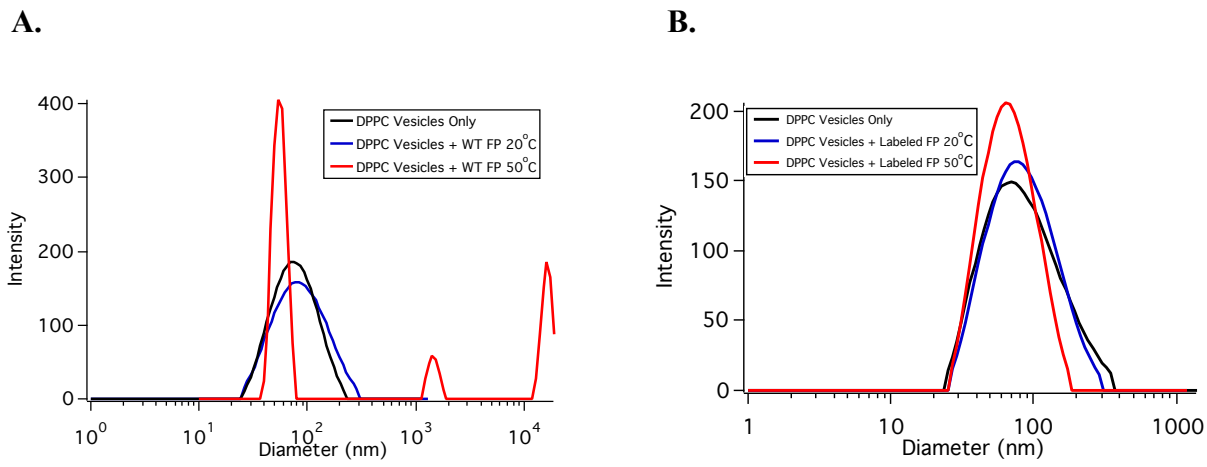

Figure 2.5. DLS of DPPC vesicles in the presence of (A) wild type fusion peptide and (B) labeled fusion peptide below and above the T_m of the membrane at 20 ^{p}C and 50 ^{o}C, respectively.

2.3.6 Estimation of Insertion Depth with FRET

Experiments were done with both C6-NBD-PC and C12-NBD-PC to compare TAMRA acceptor emission after excitation from NBD fluorescence at two different points in the bilayer. . TAMRA fluorescence emission intensity around 574 nm was monitored every 2 ^{o}C. For C6-NBD-PC, FRET emission reached a maximum intensity at 36 ^{o}C. The energy shift associated with the emission monitors changes with the environment of the N-terminus TAMRA label. The shift was fit to a sigmoid, yielding a transition at 40.8 ^{o}C, close to the T_m of the vesicles. For C12-NBD-PC, FRET emission reached a maximum intensity at 38 ^{o}C and exhibited a blue shift transition at 39.8 ^{o}C. Because FRET emission reaches a maximum intensity, indicating close proximity of the TAMRA and NBD labels, at an earlier temperature for the 6:0 label with lower overall

maximum than the 12:0 label, the data suggest that the N-terminus moves past the 6:0 location and rests closer to the 12:0 location (Figure 2.6).

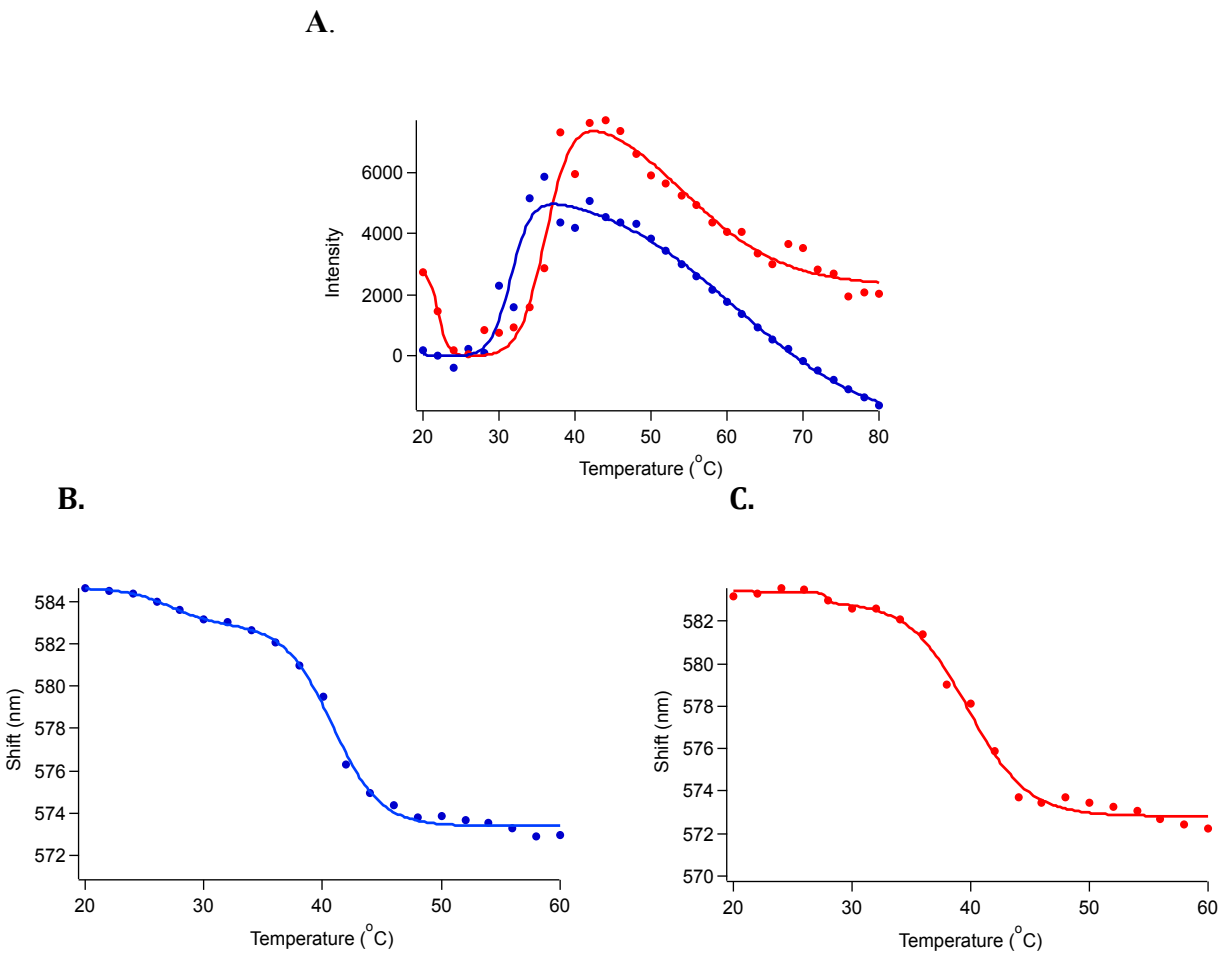

Figure 2.6. FRET emission with 460 nm excitation. (A) Comparison of temperature-dependent FRET intensities with 6:0 (blue) and 12:0 (red) NBD labels. The spectra compared with a beginning intensity of zero for a qualitative comparison of its increase upon insertion. (B) Energy shift of intensity maximum for labeled peptides in 6:0 NBD PC vesicles (C) Energy shift of intensity maximum for labeled peptides in 12:0 NBD PC vesicles.

2.4 Conclusions

This chapter aimed to detail the preliminary steps in determining the insertion depth of the hemagglutinin fusion peptide in order to move forward in studying the insertion dynamics. In this study, wild type and TAMRA-labeled FP were synthesized and purified. Analysis of both structures through CD and equilibrium fluorescence suggests the TAMRA-label does not affect the FP insertion aside from the β-sheet conformation of labeled FP in solution. In addition, labeled FP does not induce hemifusion of the vesicles as wild type FP does. The NBD labeled vesicles did not affect the structure of the vesicles; however, the hydrophobic interactions of the NBD and TAMRA fluorophores resulted in the continued insertion of the FP in the membrane following initial insertion. These results are consistent with previous studies of mutant FP studying the capacity for function correlated to structure[1]. The TAMRA label perturbs the boomerang structure the wild type fusion peptide exhibits and, therefore, cannot induce hemifusion. In summary, the fluorescent labels utilized to study peptide insertion did not alter the function of the membrane or peptide for the purpose of this experiment.

The FRET analysis of FP insertion indicates that the FP rests between the 6:0 and the 12:0 lipid chain locations in the membrane. While the original intention of studying the energy transfer between the NBD and TAMRA labels was to determine the exact peptide insertion depth in the membrane, a number of factors inhibited this goal. The intrinsic temperature dependence of the TAMRA fluorophore, exhibited in the linear decrease in intensity with temperature, and the changing dielectric constants of the environment make it difficult to resolve actual changes in intensity due to environmental changes or energy transfer. Despite these challenges, this experiment provided qualitative

evidence for the insertion depth of the fusion peptide. This data was used to develop a more precise method for both determining precise insertion depth and probing dynamics associated with insertion.

2.5 References

1. Lai, Alex L.; Freed, Jack H., The Interaction between Influenza HA Fusion Peptide and Transmembrane Domain Affects Membrane Structure. *Biophysical Journal* **2015,** *109*(12), 2523-2536.

2. Ladokhin, A. S., Measuring membrane penetration with depth-dependent fluorescence quenching: Distribution analysis is coming of age. *Biochimica Et Biophysica Acta Biomembranes* **2014,** *1838* (9), 2289-2295.

3. Chang, D. K.; Cheng, S. F.; Kantchev, E. A.; Lin, C. H.; Liu, Y. T., Membrane interaction and structure of the transmembrane domain of influenza hemagglutinin and its fusion peptide complex. *BMC biology* **2008,** *6*, 2.

4. Nagarajan, S.; Schuler, E. E.; Ma, K.; Kindt, J. T.; Dyer, R. B., Dynamics of the gel to fluid phase transformation in unilamellar DPPC vesicles. *The journal of physical chemistry. B* **2012,** *116* (46), 13749-56.

5. Schubert, T.; Schneck, E.; Tanaka, M., First order melting transitions of highly ordered dipalmitoyl phosphatidylcholine gel phase membranes in molecular dynamics simulations with atomistic detail. *The Journal of Chemical Physics* **2011,** *135* (5), 055105.

Chapter 3: Probing the Kinetics of Fusion Peptide Insertion Using Fluorescence Temperature-Jump

3.1 Introduction

3.1.1 Fusion Peptide Insertion and TMD Interaction

The previous chapter described experiments to gain a qualitative understanding of fusion peptide insertion into a membrane; however, the dynamics governing insertion is a critical component to the HA mechanism, including the timescale of insertion. FP insertion depth has been shown to affect lipid order in the membrane, a mechanism influential in promoting membrane fusion[1]. In addition, the fusion peptide interaction with the transmembrane domain is a less understood, yet vital component to the fusion mechanism. The first step in understanding this interaction is to discern the depth of insertion in greater detail and, therefore, the locations of interaction with the TMD peptide. Our attempt to discern these two mechanisms is outlined in this chapter.

3.1.2 Experimental Approach

Similar to the FRET experiments previously described, site-specific quenching has been exploited as another measure of peptide insertion depth. The decrease in efficiency caused by phospholipids containing dibrominated fatty acyl chains is due to collisional quenching. The short range of the quenching process ensures that only the lipids in its immediate vicinity of the fluorophore affect its intensity. Differential bromine labeling of the lipids provides the capability to monitor the depth of the fusion peptide[2].

Many initiation methods are available for the study of protein insertion kinetics, including laser-induced temperature-jump (T-jump). T-jump can be used to induce the membrane transition and, thus, peptide insertion on a nanosecond or microsecond timescale. Kinetics reveals that fluorescence signals change as a function of time, and the slow and fast phases report on the rates of peptide binding and insertion, respectively.

The association of a peptide to a membrane is the slowest step of the multistep process of peptide insertion, while the faster step is insertion itself. When the slowest step is the first phase of a multistep process, association and insertion cannot be independently observed. Utilizing membrane phase transitions to selectively trigger peptide insertion through rapid thermal initiation of the gel to fluid phase transition provides a unique strategy for studying the insertion of FP with temperature-jump experiments. T-jump eliminates the influence of the initial association step on dynamics measurements because the peptide is already bound to the surface before the T-jump triggers insertion. Initiating insertion this way provides sufficient time resolution to capture the dynamic process of insertion far from equilibrium[3].

3.2 Materials and Methods

3.2.1 Vesicle Preparation

DPPC, (4, 5 dibromo) PC, (6, 7 dibromo) PC, and (9, 10 dibromo) PC lipids were purchased from Avanti Polar Lipids, Inc. DPPC and brominated lipids in chloroform were mixed to generate 25 and 10 mol % vesicles. This was done for each of the three Br-labeled lipids. Preparation of lipid cakes and vesicles follows the same procedure as outlined in the Section 2.2.3.

3.2.2 Equilibrium FTIR

The same procedure as outlined in Section 2.2.4 was followed to record temperature-dependent equilibrium FTIR spectra of SUVs to analyze the transition temperatures of each vesicle mol%. Vesicles were prepared in 20 mM sodium phosphate and 100 mM sodium chloride buffer in D_2O.

3.2.3. Equilibrium Fluorescence Emission

Equilibrium fluorescence measurements followed the same procedure discussed in Section 2.2.5. Vesicles were prepared in 20 mM sodium phosphate buffer. To monitor TAMRA emission of the FP, the excitation wavelength was set to 574 nm.

3.2.4. Temperature Jump Fluorescence Spectroscopy

Time-resolved fluorescence T-jump was used to measure peptide insertion in DPPC and brominated PC vesicles. The set-up of the system has previously been described. A Ho:Nd YAG laser of 50 Hz pulsed emission is passed through an optical chopper (Thor Labs, Newton, NJ) with a 12.5 Hz repetition rate. A Verdi V12 DPSS high-power continuous wave laser (Coherent, Santa Clara, CA) is used to pump a Mira 900 Ti: Saph laser (Coherent) generating a semi-continuous 855 nm beam. The emitted fluorescence induced by a 532 nm diode laser is measured with a Hamamatsu R7518 photomultiplier tube (Hamamatsu Photonics K.K., Hamamatsu City, Japan), digitized, and signal averaged (4,000 shots) using a Tektronics model 7612D digitizer. Instrument control and data collection are controlled with a LabVIEW compouter program (National Instruments, Austin, Tx). A split IR cell composed of CAF_2 windows and 126 μM spacer consisted of the reference (peptide in buffer) and the sample (lipid vesicles and peptide in buffer). A solution of free FP in buffer was used to determine the temperature jump and temperature dependence of the TAMRA emission. A 75 μM solution of D_2O-exchanged labeled FP was prepared in 20 mM sodium acetate buffer in D_2O, pH 4 as the reference. The sample consisted of 75 μM FP and 10 mM lipid vesicles.

3.3 Results and Discussion

3.3.1 Effects of the Brominated Lipids on DPPC Structure and Phase Transition

Similar to characterizing the effects of the NBD label on DPPC vesicles, FTIR was performed on brominated DPPC SUVs to determine the effects of the label on the gel to fluid transition, as well as choose the best system to perform the quenching experiments (Figure 3.1).

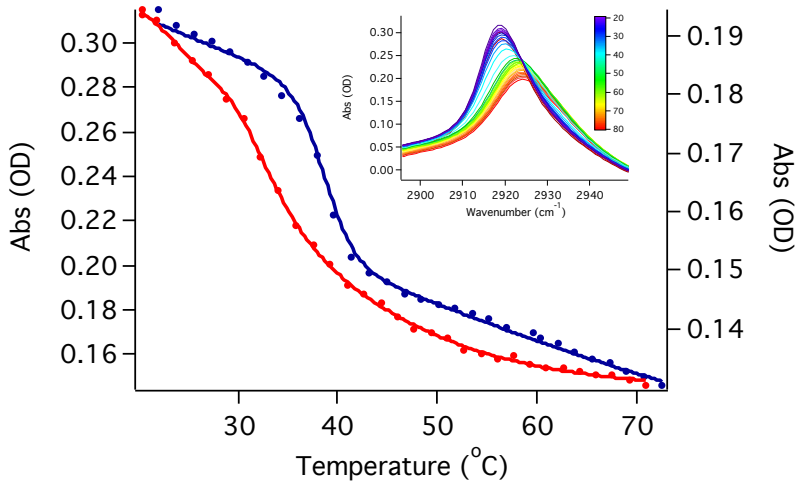

Figure 3.1. Temperature dependent FTIR spectrum (inset) and intensity vs. temperature curves of 25 mol% Br PC (red) and 10 mol% Br PC (blue) SUVs from 10-80 ^{o}C FTIR spectra portray the frequency of the CD_2 symmetric stretch. The solid lines are fit to a sigmoid to determine the transition temperatures.

Vesicles with 25 mol% and 10 mol% of probe exhibited a T_m of 34.2 ^{o}C, and 38.7 ^{o}C, respectively. In comparison to the DPPC membrane system (T_m= 41 ^{o}C), the bromine tag slightly destabilized the membrane. The 10 mol % vesicles were chosen as the best ratio to both closely resemble a DPPC vesicle and maximize the effects of bromine quenching.

3.3.2 Equilibrium Fluorescence Spectroscopy

Fluorescence emission of the labeled fusion peptide was measured at equilibrium exciting at 547 nm over a temperature range every 2 ^{o}C. Figure 3.2 shows the emission intensity maxima and energy shifts for the (6,7), and (9,10) Br-labeled vesicles.

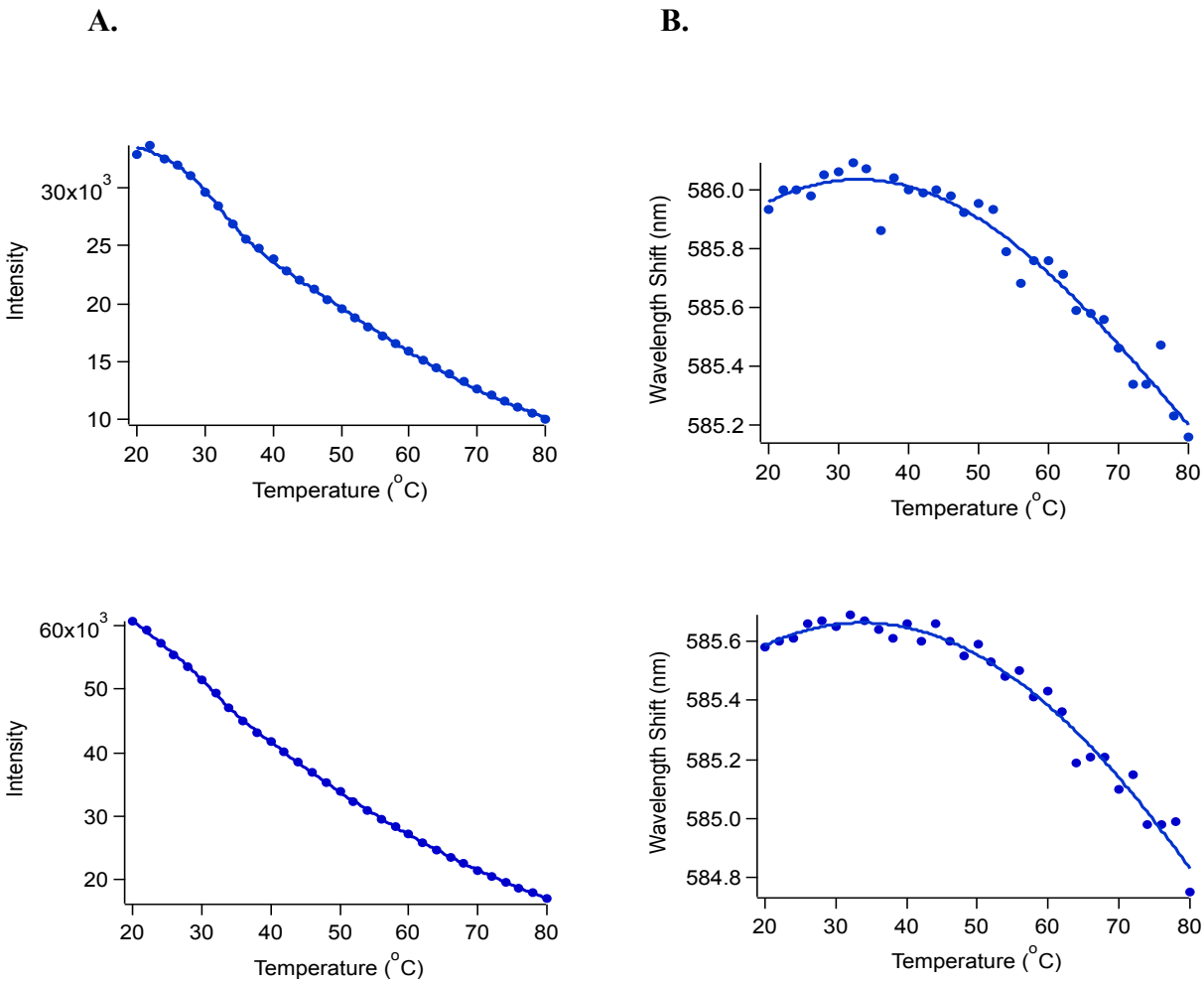

Figure 3.2. Temperature-dependent fluorescence emission from TAMRA in the labeled FP excited at 532 nm. Emission intensity maximum (left) and shift of maximum emission (right) are portrayed with (A) 6,7 Br PC vesicles and (B) 9,10 Br PC vesicles.

The data are consistent for each of the labeled vesicles. For all labeled vesicles, there is a small transition close to the T_m near 38 ^oC. An increase in emission is usually exhibited upon insertion of the TAMRA label; however, a decrease is observed at the T_m This could be attributed to quenching of TAMRA by the bromine when the FP inserts; however, it could also be explained by the insertion and exit of the FP occuring on a timescale faster than equilibrium fluorescence can probe. The wavelength is initially red-shifted, then blue shifts as the temperature increases. Aggregation of the peptide after membrane insertion would explain the blue shift observed at higher temperatures. These phenomena could be resolved using T-jump.

3.3.3 Laser-induced Temperature Jump Fluorescence Spectroscopy

T-jump was utilized to probe the rate of peptide insertion. We first measured the insertion of labeled FP with DPPC (Figure 3.3).

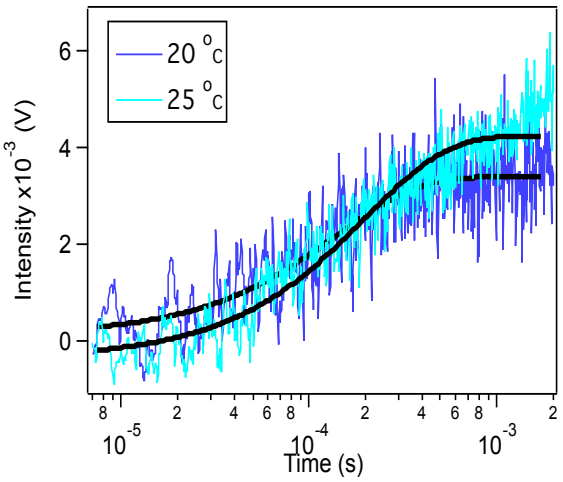

Figure 3.3 Temperature-jump of TAMRA-labeled FP in DPPC starting at 20 and 25 ^oC. Lifetimes (τ) are 141 and 200 μsec, respectively.

We then measured the insertion of labeled FP with (4,5) Br, (6,7) Br, and (9,10) Br PC vesicles to determine the effect of quenching on TAMRA fluorescence as the peptide inserts into the membrane (Figure 3.4).

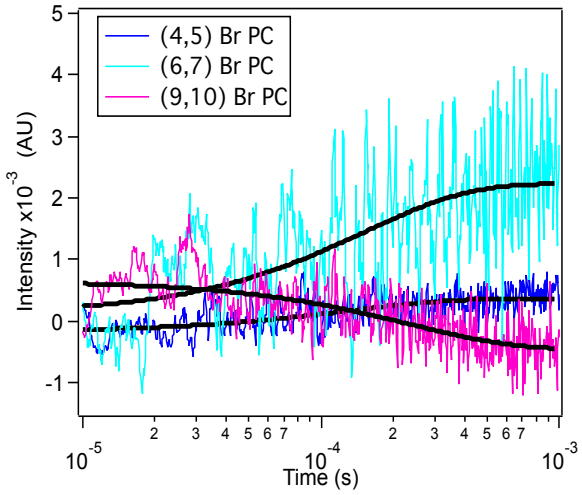

Figure 3.4 Temperature-jump of TAMRA-labeled FP in brominated vesicles starting at 25 ^{o}C.

In order to compare FP insertion in DPPC with insertion in brominated lipids, the competing and opposite effects on the signal from increase in emission due to insertion and bromine quenching must be considered. The net change in signal depends on the location of the bromine label. Compared to FP insertion in DPPC, only the 9,10 Br vesicles results in a negative signal, indicating that the quenching effect dominates the insertion signal. This suggests that the TAMRA is located at least this deep in the

membrane. The positive signals for the 4,5 and 6,7 Br vesicles result from TAMRA quickly bypassing the more shallow levels and only exhibiting an increase in signal from insertion. The rate of insertion and subsequent interaction with the bromine label decreases with the depth of the bromine label in the membrane, with rates of 130, 153, and 236 μsec, respectively. Because the signal continues to exhibit lower amplitude than that with DPPC even at the 9,10 Br location, the peptide likely inserts past this depth.

We also measured W14A mutant of H3N2 FP, probing the tryptophan in the middle of the FP structure. The rate for the labeled FP, labeled at the N-terminus, is faster. This is consistent with other evidence that the FP follows vectorial insertion in the membrane, with the N-terminus preceding the rest of the FP.

3.4 Conclusions

Probing the insertion depth and dynamics of the fusion peptide is important for facilitating the study of the fusion peptide and its role in membrane fusion. We are utilizing lipid-attached bromine quenchers to monitor membrane penetration with temperature-jump spectroscopy. We were able to gather preliminary data that will serve as the foundation for further experimentation using this approach. It was shown that quenching of TAMRA fluorescence is occurring as the N-terminus inserts into the membrane. The insertion of the FP is deep in the membrane, likely to at least the 10-C on the 16-C lipid chain. The rate of insertion is on the μsec, timescale. This study was complicated by the low bromine content (1 mol%), chosen so as to not perturb the membrane. As a result, it is difficult to resolve the simultaneous and competing increase in signal due to desolvation of the fluorophore and decrease due to quenching.

3.5 References

1. Lai, Alex L.; Freed, Jack H., The Interaction between Influenza HA Fusion Peptide and Transmembrane Domain Affects Membrane Structure. *Biophysical Journal* **2015,** *109* (12), 2523-2536.

2. Ladokhin, A. S., Measuring membrane penetration with depth-dependent fluorescence quenching: Distribution analysis is coming of age. *Biochimica Et Biophysica Acta Biomembranes* **2014,** *1838* (9), 2289-2295.

3. Nagarajan, S.; Schuler, E. E.; Ma, K.; Kindt, J. T.; Dyer, R. B., Dynamics of the gel to fluid phase transformation in unilamellar DPPC vesicles. *The journal of physical chemistry. B* **2012,** *116* (46), 13749-56.

Chapter 4: Probing the Dynamics of the Gel to Fluid Phase Transition in Unilamellar DPPC Vesicles Through Aggregation of NBD

4.1 Introduction

The dynamics of the gel to fluid phase transition of lipid bilayers is less understood than the structure or thermodynamics of the phases. Previous studies have utilized laser temperature jump coupled with time-resolved infrared spectroscopy to directly follow the dynamics of the gel to fluid phase transition through acyl change structural changes[1]. In this work, we are utilizing the self-association of dye in a lipid bilayer to probe gel to fluid phase transition dynamics and further our understanding of this event.

J-aggregates of many dyes and aromatic compounds have been extensively investigated and are the result of tightly packed dye molecules associating due to strong intermolecular dispersion forces between the molecules. The molecules form a "head-to-tail" transition dipole arrangement that generates a split excitonic state[2]. It is characterized by a bathochromic shift, or red shift, compared to the monomer[3] (Figure 4.1).

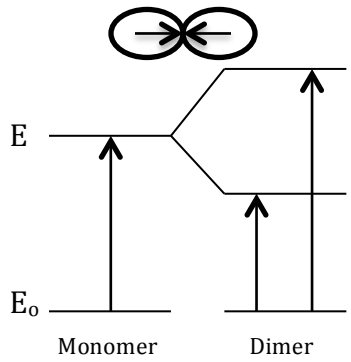

Figure 4.1 Representation of the relationship between the head-to-tail arrangement of molecules and the associated spectral shift.

Equilibrium fluorescence spectroscopy is sensitive to the formation of J-aggregates due to the unique spectral signature of the J-aggregates. The labeled lipids segregate in the gel phase and disperse in the fluid phase, so the spectra can be used to follow the dynamics of the phase transition and subsequent dispersal. T-jump can follow this change on time scales associated with the fast phase transition. The rapid aggregate to monomer transition is triggered with temperature, so resolving the time-scale of the transition adds another layer of understanding the dynamic organization of membranes.

4.2 Materials and Methods

4.2.1 Vesicle Preparation

Vesicles were prepared following the protocol outlined in Section 2.2.3. DPPC and 6:0 NBD PC lipids in chloroform were mixed to generate 15% and 1% NBD PC vesicles.

4.2.2 Equilibrium Fluorescence Emission

Equilibrium fluorescence measurements followed the same procedure discussed in Section 2.2.5. Vesicles were prepared in 20 mM sodium phosphate buffer. To monitor NBD emission, the excitation wavelength was set to 460 nm.

4.2.3 Temperature Jump Fluorescence Spectroscopy

Time-resolved fluorescence T-jump was used to monitor the aggregate to monomer transition of NBD-labeled vesicles. The reference and sample were 10 mM solutions of 1 mol% and 15 mol% NBD PC vesicles, respectively.

4.3 Results and Discussion

4.3.1 Equilibrium Fluorescence Detection of J-Aggregation

The temperature-dependent fluorescence of NBD in vesicles is shown in Figure 4.2A. The spectrum shows the emission from excitation at 460 nm over a temperature range of 10-80 ^{o}C. The fluorescence emission spectrum clearly indicates a sharp increase in ntensity at 37^{o} and blue shift at 35 ^{o}C.

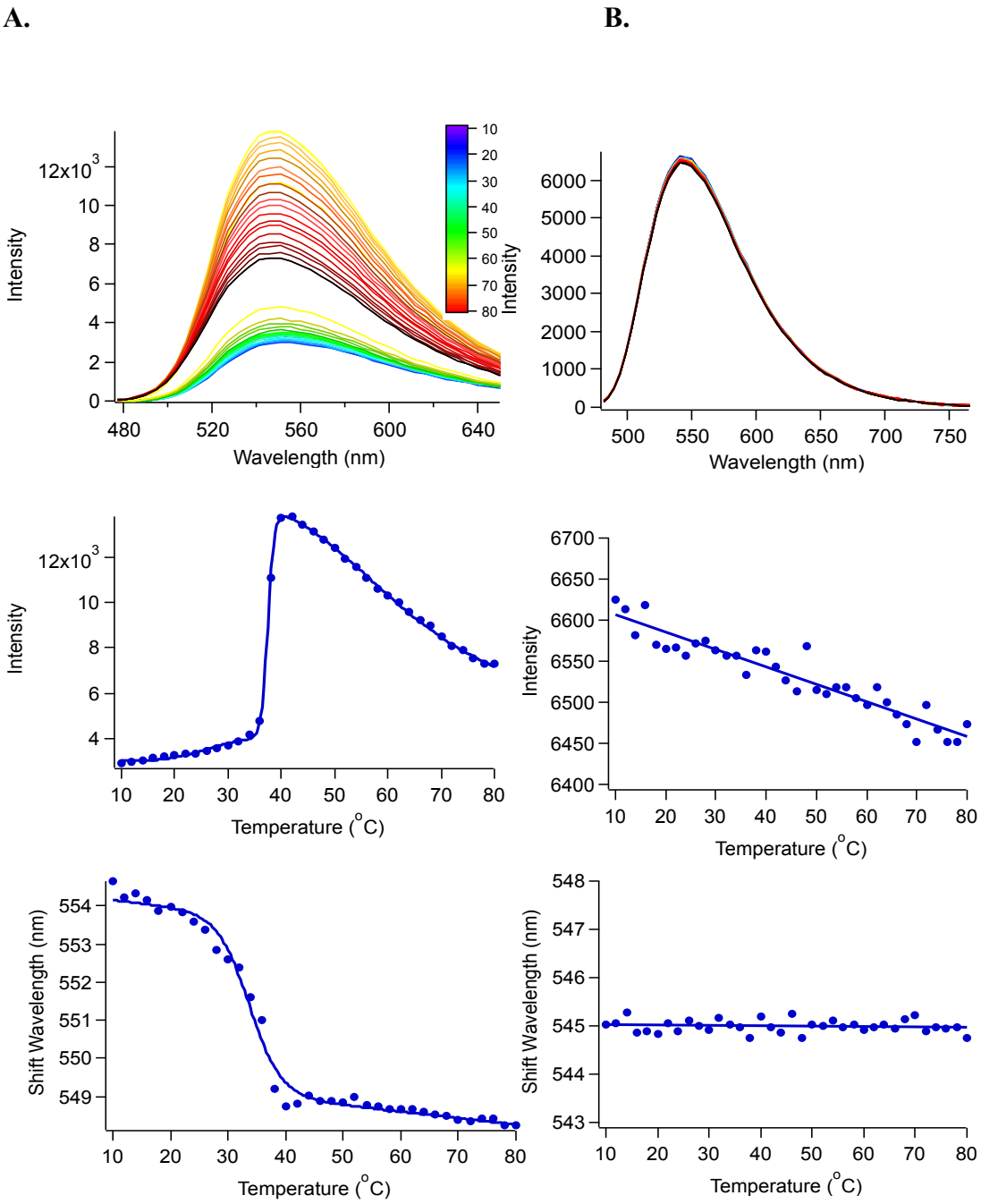

Figure 4.2. Comparison of the temperature-dependent fluorescence spectra of 15 mol% (A) and 1 mol% (B) NBD PC vesicles excited at 460 nm.

The emission spectrum of 1 mol% NBD PC vesicles is characterized by a homogeneous distribution of the dye in the vesicles throughout the membrane phase changes (Figure 4.2B). The intensity decreases linearly with temperature due to the intrinsic temperature dependence of NBD, and no energy shift is associated with the phase change. Comparing the 15 mol% and 1 mol% spectra clearly indicates that that NBD-labeled lipid distribution is sensitive to the composition of SUVs formed from DPPC.

The gel phase is characterized by a red-shift and increased intensity, due to the J-aggregation of NBD, relative to the monomer signal in the fluid phase. The NBD aggregation is enhanced by the rigid membrane structure and causes quenching of the fluorescence signal; in the fluid phase, lipids move more freely in the membrane, and the lipids become less phase-segregated and, therefore, unquenched (Figure 4.3).

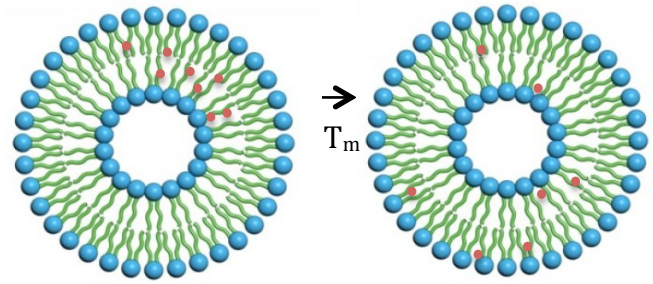

Figure 4.3. Scheme of deaggregation of NBD lipids in DPPC vesicles as the membrane undergoes a gel to fluid phase transition.

These results indicate the deaggregation of NBD with the membrane phase transition, making J-aggregation in vesicles useful for probing phase transitions of SUVs.

4.3.2 Temperature Jump Fluorescence Spectroscopy of NBD J-Aggregation

Laser-induced temperature-jump fluorescence spectroscopy can be utilized to study the dynamics of the gel to fluid phase transformation of small unilamellar vesicles, and we have gathered preliminary data for this experiment. It has been shown that this transformation in response to a large T-jump perturbation is fast (submicrosecond timescale). One of the limitations of this experiment is the small intrinsic temperature dependence of NBD fluorescence emission, which makes the jump difficult to monitor; however, we should be able to utilize this approach to monitor phase transition dynamics.

4.4. Conclusions

We have begun to resolve the association of the deaggregation of NBD lipids in DPPC small unilamellar vesicles with the main gel to fluid phase transition. The phenomenon is dependent on membrane composition, evident when comparing 15 mol% and 1 mol% of NBD in DPPC vesicles. Fluorescence emission is sensitive to this change, triggered by temperature, and can be monitored at both equilibrium and dynamically. Because the fundamental dynamics of the phase transition occur on the submicrosecond timescale and fluidity plays a role in the aggregation process, it is likely that the aggregate to monomer transition is just as fast.

4.5 References

1. Nagarajan, S.; Schuler, E. E.; Ma, K.; Kindt, J. T.; Dyer, R. B., Dynamics of the gel to fluid phase transformation in unilamellar DPPC vesicles. *The journal of physical chemistry. B* **2012,** *116* (46), 13749-56.

2. (a) Jelley, E. E., Spectral Absorption and Fluorescence of Dyes in the Molecular State.

Nature **1936,** *138*, 1009-1010

(b) Yao, H.; Omizo, M.; Kitamura, N., Mesoscopic string structures of thiacyanine J aggregates in solution. *Chemical Communications* **2000,** (9), 739-740

(c) Sidorowicz, A.; Mora, C.; Jabłonka, S.; Poła, A.; Modrzycka, T.; Mosiądz, D.; Michalak, K.,Spectral properties of two betaine-type cyanine dyes in surfactant micelles and in the presence of phospholipids. *Journal of Molecular Structure* **2005,** *744–747*, 711-716.

3. Norland, K.; Ames, A.; Taylor, T., SPECTRAL SHIFTS OF AGGREGATED SENSITIZING DYES. *Photographic Science and Engineering* **1970,** *14* (5), 295 .

Chapter 5: Conclusions and Perspectives

This thesis aims to study an aspect of dynamic protein-membrane interactions, specifically the role of peptides in membrane fusion. Previous studies have examined the structure of influenza hemagglutinin fusion peptide extensively and are beginning to investigate the mechanisms of the peptide in relation to the fusion process; however, many questions remain regarding the time-resolved dynamics of insertion and the TMD-FP interaction. Understanding these dynamics and interactions is crucial to understanding the role of hemagglutinin in the membrane fusion process.

To begin to address these questions, we performed mechanistic investigations to determine the insertion depth and rate of the fusion peptide in a membrane using fluorescence spectroscopy couple to temperature-jump. Temperature-jump offers the time resolution necessary to capture this dynamic insertion. We first successfully established and optimized an approach to probe depth through peptide labeling with TAMRA and membrane labeling with NBD in Chapter 2. We found that the fluorescence labels to no significantly perturb the system for the purpose of our studies. Using FRET between the peptide and lipid labels, we determined that the peptide inserts between the C6:0 and C10:0 position in the membrane. This study provided qualitative evidence for fusion peptide insertion depth; however, FRET was not a sufficient method for determining exact depth due to other factors that contribute to fluorescence emission, including the dielectric of the solvent and intrinsic temperature dependence of the fluorophores. In addition, equilibrium studies provide only a static analysis of a dynamic mechanism.

In Chapter 3, we continue the study of FP insertion through dynamic studies with temperature-jump spectroscopy. We utilized depth-dependent fluorescence quenching with brominated lipids to probe insertion depth. Though the results are preliminary and

only skim the surface of experiments needed to be done, we found that the bromine quencher lowers the amplitude of fluorescence signal for the 9,10 vesicles, indicating that the TAMRA label is inserted this deeply in the membrane. In addition, the lifetime associated with each labeled depth corerlates directly with depth. The lifetime increases as the bromine quencher is located more deeply in the membrane. In addition, we were able to gather evidence of vectorial insertion of the fusion peptide starting with the N-terminus. We will continue to optimize this experiment to gather cleaner data with more signal. We used only 1 mol% of brominated lipids in these experiments. The low effects of quenching combined with the high intensity increase from insertion results in competing signals that cancel each other out during the insertion. Experiments should be done with an increased concentration in bromine quenchers. This will provide more substantial evidence for FP depth and rate of insertion.

Chapter 4 interrogates the J-aggregation of NBD label in DPPC membranes. We found that the desegration of the J-aggregates in high NBD composition membranes occurs in association with the gel to fluid phase transition of the membrane, which provides method for further studying the dynamics of the transition. We predict that desegregation occurs on a similar timescale to the phase transition. This experiment is difficult to conduct due to the small intrinsic temperature dependence of the NBD fluorophore. T-jump experiments at the T_m need to be conducted to obtain the transition rate.

It is important to note that these studies were conducted in model membranes of varying sizes, which may have affected the conformation of the fusion peptide. In addition, the isolated peptides may have different energetics and fusogenic behaviors than

the intact hemagglutinin protein. These limitations should be considered when drawing conclusions regarding the hemagglutinin system.

These experiments were designed to ultimately facilitate the study of the fusion peptide and its interaction with the transmembrane domain to investigate their role in the membrane fusion process. Further experimentation will be required to gather conclusive evidence for fusion peptide insertion mechanisms and dynamics. After this data is obtained, it can be used to predict the points of interaction of FP with TMD, with which the peptides can be labeled to monitor the dynamics of this interaction.